Chen et al. Advances in Bridge Engineering (2021) 2:11
https://doi.org/10.1186/s43251-020-00031-6

Advances in Bridge Engineering

ORIGINAL INNOVATION Open Access

Damage control of a twin-column pier with a replaceable steel shear link in a cap beam under transverse seismic motion

Weiting Chen[1], Xuemeng Bai[2], Tengfei Xu[1,3], Shanshan Ke[1], Kailai Deng[1,3*] and Haiqing Xie[4]

* Correspondence: kailai_deng@163.com
[1]Department of Bridge Engineering, Southwest Jiaotong University, Chengdu 610031, China
[3]Sichuan Province Key Laboratory of Seismic Technology, Southwest Jiaotong University, Chengdu 610031, People's Republic of China
Full list of author information is available at the end of the article

Abstract

This paper proposes a novel twin-column pier with a steel shear link (SSL) installed in the cap beam to reduce seismic damage in the transverse direction. The SSL interrupts the rigid cap beam and relieves the coupled deformation of the two columns. Benefits of the yieldable SSL in the event of a strong earthquake are the longer effective deformation of a column and limited axial compressive load. A benchmark reinforced-concrete bridge is employed in a seismic performance evaluation to verify the damage reduction performance of the novel twin-column pier with an SSL. Five numerical models, calibrated in a physical component test, are built in ABAQUS; that is, one original bridge and four novel bridges with different SSLs and accompanying configurations. Modal analysis shows that introducing the SSL does not change the overall structural dynamic characteristics. The nonlinear dynamic analysis results indicate that adopting the SSL effectively reduces the peak compressive strain of the reinforced-concrete column, but energy dissipation from the SSL is negligible compared with the total inputted seismic energy. There is no evident change in the macro seismic response of the twin-column pier when using the SSL, such as overall drift and structural damping ratio. Moreover, a transverse continuous main girder is suggested for realizing an additional restoring moment at the column top, which further reduces compressive strain.

Keywords: Twin-column pier, Steel shear link, Decoupled deformation, Dynamic analysis, Damage reduction

1 Introduction

Well-designed reinforced-concrete (RC) bridges have avoided collapse during earthquakes in recent years but RC piers have still suffered severe damage, for which rehabilitation is difficult (Bhuiyan and Alam 2013; Ishibashi and Tsukishima 2009; Han et al. 2009). In the case of a twin-column pier of a beam bridge, the strong cap beam constrains columns in the transverse direction. The twin-column pier behaves similarly to a portal frame under transverse seismic excitation according to the 'strong-beam weak-column' design principle, as shown in Fig. 1.

The strong-beam weak-column mechanism evidently reduces the effective deformation length of the column. Plastic hinges usually appear at the column bottom.

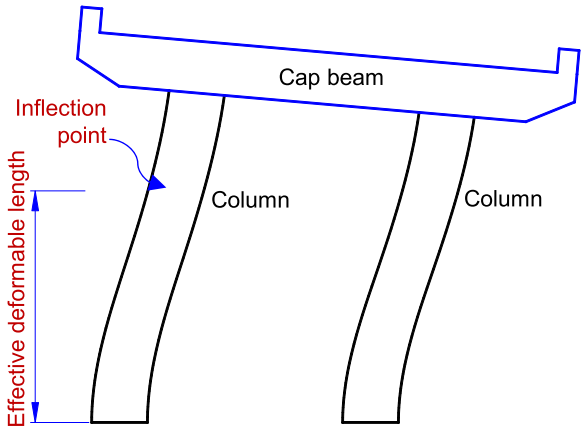

Fig. 1 Deformation pattern of a twin-column pier of a beam bridge under transverse seismic motion

Moreover, owing to the frame effect, the axial compressive force acting on one column must increase while that acting on the other column decreases. The fluctuating axial load may cause compressive damage, even crushing of the RC column, for which repairs are difficult (Deng et al. 2019b).

The frame-type damage mode of twin-column piers was observed for the Wenchuan earthquake (Zhuang and Chen 2013)). Many twin-column piers suffered severe damage to the column bottom and even collapsed through over-turning. Many scholars have installed dampers between the girder and pier to reduce the overall seismic response (Shen et al. 2017; Taflanidis 2011). The dampers and bearings are usually designed with a low shear load resistance and large deformation capacity for early yielding and excellent energy dissipation (Deng et al. 2014b). However, the girder–pier relative displacement must be small to avoid failure as a result of a girder falling. Stoppers in the transverse direction, even ductile stoppers, still transfer a huge horizontal load to twin-column piers. It would otherwise not be possible to prevent failure through a girder falling (Xu and Li 2014). On the basis of the frame-type deformation characteristics of the twin-column pier, Dong et al. (2017) diagonally placed a self-centering buckling restrained brace (SC-BRB) between two columns. With the strong cap beam, the twin-column pier presented obvious horizontal shear deformation, such that the diagonally placed SC-BRB effectively dissipated energy and reduced residual deformation. For a twin-column pier with a minimal distance between columns, El-Bahey and Bruneau (2012) experimentally studied the effect of different structural fuses installed between the two columns. The twin-column pier with fuses exhibited stable hysteretic performance with little pinching. However, the rigid cap beam on the twin-column pier still limited the ultimate deformability of the pier. According to recent progress in building engineering, the approach of structural control design has become available for reducing seismic damage. Deng et al. (2019a) installed a steel–ultra-high-performance-concrete composite joint at a beam end to tolerate large deformation and protect the column from plasticity. Ji et al. (2017) developed a hybrid coupled wall system with replaceable steel coupling beams, which was designed as an early-yielding component that limits the axial force in the walls and has good energy dissipation. Mansour (2010) employed replaceable shear links in eccentrically braced frames. These links transferred plastic deformation from the connection zone to the middle of the beam. The overall

deformation mode changed such that the main structural components (i.e., the steel beam and column) remained elastic. To this end, structural control design is an effective approach for reducing damage in a seismic event.

This paper proposes a novel twin-column pier with a replaceable steel shear link (SSL) in the middle of the cap beam. This design is expected to change the overall deformation mode of the twin-column pier and dissipate energy under transverse seismic excitation. The RC columns are well protected from seismic damage owing to the deformation control and additional energy dissipation. After an earthquake, the SSL can be easily replaced through a bolting connection. To verify the damage control performance of the novel twin-column pier, nonlinear dynamic analysis is conducted for a three-span simply-supported beam bridge. Seismic responses (i.e., the transverse deformation, curvature distribution, and strain development) are observed. Numerical analysis results show the realized performance of damage control of the novel twin-column pier with the SSL. The effects of design parameters of the novel twin-column pier are discussed.

2 Concept of a twin-column pier with a steel shear link

The structure and expected deformation mode of the novel twin-column pier with an SSL are shown in Fig. 2. The SSL is installed in the middle of the cap beam, which is expected to withstand large shear deformation and dissipate energy under transverse seismic excitation. The SSL releases the completely coupled deformations of the two columns and enlarges the effective deformable length of the two columns. Compared with conventional twin-column piers, the novel twin-column piers experience much less sectional curvature at the column bottom when subjected to the same transverse drift at the pier top. Furthermore, the yielding strength of the shear link is the essential upper bound of the earthquake-exerted axial compressive force for one column. Compressive damage to the RC columns can be avoided by selecting the yielding strength of the SSL.

However, the decoupled deformation of the two columns, as well as their cap beams, is not coordinated with the deformation of the main girder. In an earthquake, the gravity of the main girder is not uniformly shared by the bearings, resulting in an amplified load-carrying capacity demand of bearings. The continuity of the main girder in the transverse direction is taken as a parameter in the following analysis.

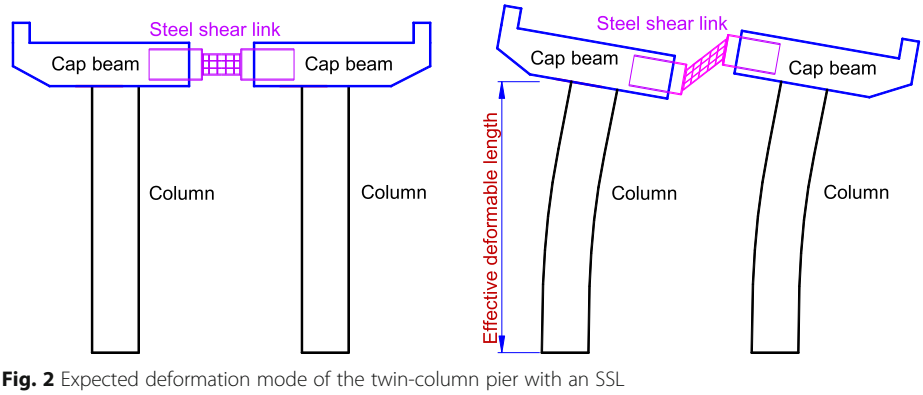

Fig. 2 Expected deformation mode of the twin-column pier with an SSL

3 Benchmark continuous-beam bridge

A typical three-span simple-supported beam bridge from the practical engineering is employed to verify the performance of seismic damage control as shown in Fig. 3. Each span has a length of 30 m. The main girder comprises four pre-stressed concrete box beams placed side by side and connected by a delay-casted closure pour. The two ends of the main girder have diaphragms with thickness of 500 mm. The two RC columns have a height of 8.0 m and a separation of 6.3 m. The cap beam is made of pre-stressed concrete, with a reinforcement ratio of 2.4%. The cross section of the rectangular RC column is also presented in Fig. 3. The sectional reinforcement ratio is 1.8%. Four polytetrafluoroethylene (PTFE) slide bearings and four elastomeric pad (EP) bearings are used on the abutments and twin-column piers respectively. The friction coefficients of the PTFE slide bearing and EP bearing are 0.03 and 0.3 respectively (MCPRC 2004). Note that there is one fixed bearing in transverse direction at one end of the main girder.

Three novel twin-column piers are designed on the basis of the original pier (denoted O1), as shown in Fig. 4. The connecting beam and overall dimensions of the SSL are the same for the four novel piers. The SSL has a length of 450 mm and height of 232 mm. The flanges have a thickness of 32 mm, which guarantees the required bending capacity. The SSL is connected to the cap beam through one large I-shaped steel beam. One end of the steel beam is embedded in the cap beam while the other end is bolted to the SSL. The connecting steel beam should remain elastic in an earthquake, and all the plasticity concentrates on the SSL. The benefit of the bolting connection is that the SSL can be quickly replaced after an earthquake. The design of the connecting steel beam, including the embedded length, profile of the steel beam, and bolting connection, can follow the design of the steel coupling beam in a hybrid wall system (El-Tawil et al. 2010). The widths of the SSL and connecting steel beam are each 200 mm. The differences between the four novel piers are the web thickness of the SSL and transverse continuity of the main girder. The SSL has the thickness of the web. 30C has a web thickness of 30 mm and a continuous main girder. 8C has a thinner web of just 8 mm. 30D and 8D have a main girder discontinuous in the transverse direction and a

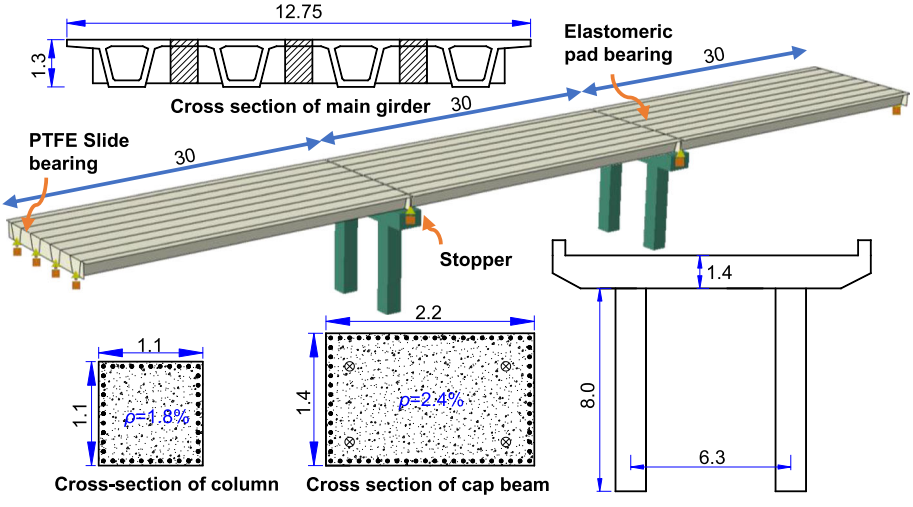

Fig. 3 Structures of the benchmark simply-supported beam bridge (unit: m)

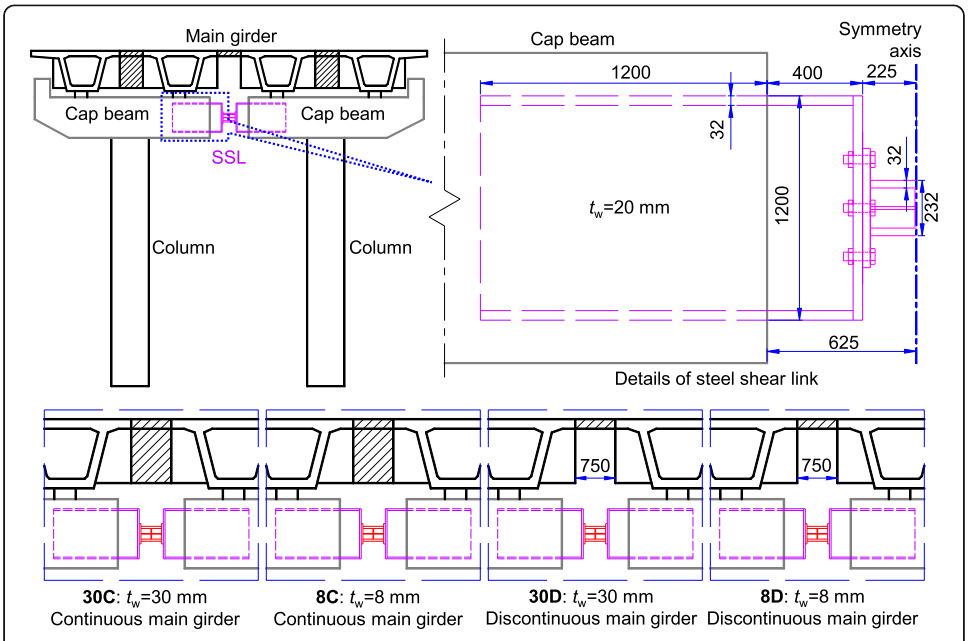

Fig. 4 Design of the novel twin-column pier with an SSL (unit: mm)

30-mm thick and 8-mm thick SSL respectively. The parameters of the models were summarized in Table 1.

Material information is given in Table 2. C50 and C30 concrete, having compressive strengths of 32.4 and 23.4 MPa, are applied for the main girder and twin-column pier respectively. The yielding strengths of HRB400 rebar and LY225 steel are respectively 400 and 225 MPa.

3.1 Modeling in ABAQUS

Finite element models are built in ABAQUS, as shown in Fig. 5. The main girder and SSL are simulated with shell elements while the cap beam and columns are simulated with Timoshenko beam elements. The main girder, made of pre-stressed concrete, reminded elastic during the earthquake. For simplistic calculation, only elastic material property was applied to the main girder.

For the RC twin-column pier and cap beam, the uniaxial confined concrete strain-stress relationship was applied, which ignored the tensile strength. The ascending part developed as parabolic curve. Once achieving the peak confined strength f_c, the stress linearly deteriorated until the ultimate strength f_u, i.e. 0.2 × f_c. Then, the compressive

Table 1 Design of the twin-column pier

Model	Category	Thickness of SSL web /mm	Continuity of main girder
O1	Original design	--	Continuous
30C	Using SSL	30	Continuous
8C	Using SSL	8	Continuous
30D	Using SSL	30	Discontinuous
8D	Using SSL	8	Discontinuous

Table 2 Material properties and applications

Material	Nominal strength	Applied components
C50 concrete	$f_c = 32.4$ MPa	Main girder
C35 concrete	$f_c = 30.5$ MPa	Twin-column pier (considering the confinement from stirrup)
HRB400 rebar	$f_y = 400$ MPa	Main girder & Twin-column pier
LY225 steel	$f_y = 225$ MPa	Connecting steel beam, SSL

Remark: f_c is the compressive strength of concrete while f_y is the yielding strength of rebar and steel

stress keeps constant when subjecting to the further compressive strain. The values of characteristic performance points, i.e. (ε_c, f_c), (ε_u, f_u), were calculated from Saatcioglu Model (Saatcioglu and Razvi 1992).

As for the reinforcement in the RC piers, a load-path dependent hysteretic model is used. The constitutive law of HRB400 rebar obeys the Clough model with the kinematic hardening. When subjected to the reversing loading, the stress-strain curve pointed to the $0.2\sigma_{max}$ with the unloading stiffness. Then the strain-stress curve points to the peak value (σ_{max}, ε_{max}) in history with reduced stiffness until achieving yielding stress (Gao and Zhang 2013). This model was very effective to reproduce the pinching effect in the reinforced concrete structure under large deformation (Deng et al. 2019b).

The LY225 steel for SSL follows an exponential hardening law after a yielding strength of 225 MPa. Before initial yielding, the strain-stress relationship is linear. When the strain is up to the inimical yielding strain, the kinematic hardening stress α of LY225 steel is calculated as Eq. (1), where $\bar{\varepsilon}^{pl}$ is the cumulative plastic strain (*CPS*) and C_k and γ_k are parameters of the model (Abaqus 2015).

$$\alpha = \sum_{k=1}^{n} \frac{C_k}{\gamma_k} \left(1 - e^{-\gamma_k \bar{\varepsilon}^{pl}}\right) \tag{1}$$

The bearings and restrainers are respectively modeled with a nonlinear connector and gap element. An ideal elastic–plastic model is applied to the bearings. The yielding forces are the product of the gravity load and friction coefficients. For this bridge, the yielding forces of the PTFE slide bearing and EP bearings are respectively 30.2 kN and 302 kN. The fixed bearings had no yielding force, just provide the linear displacement-force relationship.

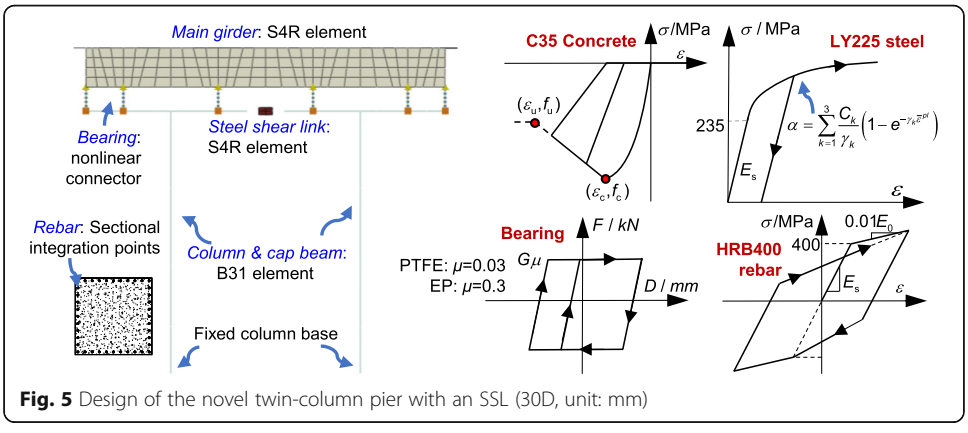

Fig. 5 Design of the novel twin-column pier with an SSL (30D, unit: mm)

In the case of the novel twin-column pier, the connecting steel beam is not explicitly built in the model. The connecting steel beam must remain elastic in an earthquake owing to its much larger capacity relative to the SSL. Multiple-point constraints are thus used to connect the side stiffener of the SSL with the neighboring nodes of the cap beams.

3.2 Model verification

The modeling strategy is verified using the previous test results for the RC column and SSL. A typical RC column experienced the cyclic deformation was used to verified the constitutive material model of confined concrete and reinforcement (Li 2010). The tested circular RC column had the height of 2300 mm and diameter of 400 mm. 12 HRB400 rebars with the diameter of 14 mm were used. A beam element-based model was built to reproduce the hysteretic behavior of the RC column. The modeling strategy and material properties exactly follows the above statement. According to Fig. 6a the numerical model delivered good agreement with the test results. This comparison proved the effectiveness of the concrete and reinforcement models.

Deng et al. (2014a) provided a test the steel shear panel damper made of LY225 steel, which was used for the model verification. The shear panel damper subjected to the cyclic loading under different amplitudes. A shell element based model was built in ABAQUS, as shown in Fig. 6b. The parameters in the constitutive material model (Eq. (1)) of LY 225 steel was presented in Table 3. By applying the same load protocol, the numerical model could well reproduce the hysteretic behavior of the steel shear panel damper, demonstrating the practicability of the material model for LY225 steel.

3.3 Ground motion records

Seven ground motions (GMs) are selected from the Pacific earthquake engineering research center database by fitting the design response spectrum, as shown in Fig. 7a. Figure 7b compares the response spectra of the seven GMs with the target spectrum, showing good agreement. In the nonlinear dynamic analysis, GMs are input in

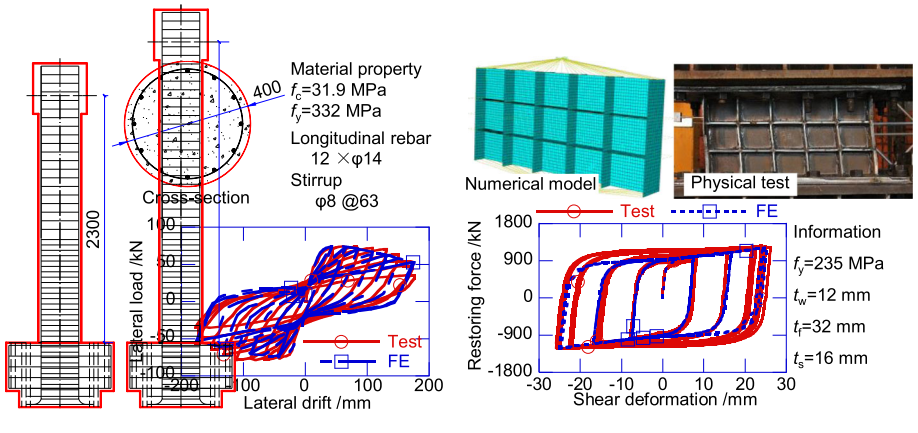

(a) Cyclic test of the RC column (b) Cyclic test of the SSL

Fig. 6 Verification of the modeling strategy (Li 2010; Deng et al. 2014a)

Table 3 Parameters of the numerical material law

f_y/MPa	C_1/MPa	γ_1	C_2/MPa	γ_2	C_3/MPa	γ_3
235	20,000	400	18,000	500	1200	2

transverse and vertical directions at the same time. The vertical component is 0.65 times the transverse component. The seismic fortification intensity is 8 degrees for the bridge according to the Chinese seismic design code [14]. This intensity corresponds to peak ground motion accelerations (PGAs) of 0.07 g, 0.2 g, 0.4 g, and 0.51 g for a service level earthquake (SLE), design-based earthquake (DBE), maximum considered earthquake (MCE), and very rare earthquake (VRE) respectively.

4 Modal analysis

Modal analysis is first performed. The use of the SSL does not affect the vibration modes or frequencies in the longitudinal direction. The first and second vibration periods in the transverse direction are presented in Table 4. Even with the 8-mm thick SSL, only 1.9 and 0.8% elongations are observed for the first and second modes, respectively. Similar to the coupled shear wall, the lateral stiffness of the twin-column pier was mainly controlled by the sectional size and height of the RC column. The thickness of the SSL didn't evidently affect the vibration periods. Compared with 30C and 8C, 30D and 8D have larger natural periods in the transverse direction. The continuous main girder contributes to the transverse stiffness of the bridge.

5 Dynamic analysis results

5.1 Deformation and damage mode

The representative overall deformation modes of two twin-column piers are compared in the left part of Fig. 8. All piers deliver a similar overall deformation mode; that is, reinforcement yielding at the bottom of two RC columns at MCE intensity. However, the inflection point cannot be eliminated by introducing the SSL in the cap beam, even in the case of the 8-mm thick SSL. The right part of Fig. 8 shows the representative curvature distribution along the left column. The curvature concentrates at the top and bottom of the column. Note that O1 experiences slightly larger curvatures at the column top compared with novel piers with the SSL, indicating the relief of the inflecting deformation of the columns. Meanwhile, the five models have similar curvature at the bottom of the RC column.

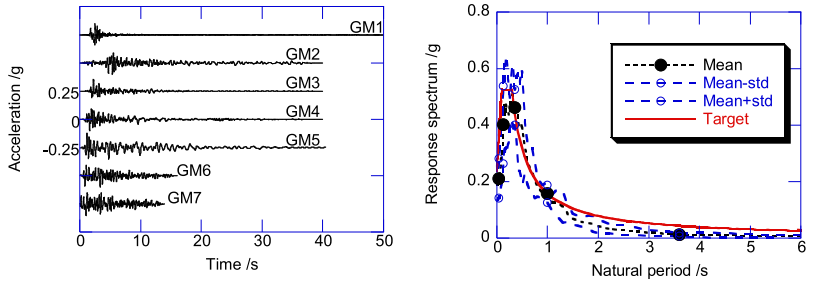

(a) Seven GM records (b) Response spectra

Fig. 7 Selected GMs and response spectra

Table 4 Vibration periods in the transverse direction (Unit: s)

Model	1st mode	2nd mode
O1	0.599	0.443
30C	0.604	0.445
8C	0.611	0.447
30D	0.627	0.459
8D	0.635	0.461

Figure 9 presents the damage status, namely the yielding of the SSL and yielding of RC columns, at all intensities. At the SLE intensity, the SSL yields only for 8D. No column yields at the SLE intensity, indicating the good design of the RC bridge. At MCE and VRE intensities, the SSL and RC columns yield for all GMs. This result primarily demonstrates the damage control performance at the DBE intensity.

The maximum transverse drift ratios (DRs) of columns are presented in Fig. 10. The five models have similar maximum DRs regardless of the earthquake intensity. It is concluded that adopting the SSL does not affect the transverse deformation response of twin-column piers.

The residual DRs of twin-column piers are presented in Fig. 11. At SLE and DBE intensities, the residual DRs didn't have evident difference. At MCE intensity, adopting the SSL could result in the smaller DRs. The continuity of main girder and thickness of SSL webs didn't affect too much on the residual DRs at MCE intensity. While at VER intensity, the twin-column piers with discontinuous main girder had larger residual DRs. But 30C and 8C had smaller residual DRs. The yielding of SSL and RC columns are irrecoverable deformations. Thus, the residual DRs are very discrete, depending heavily on the characteristics of GMs. In general sense, using SSLs didn't increase the residual deformation of the twin-column piers.

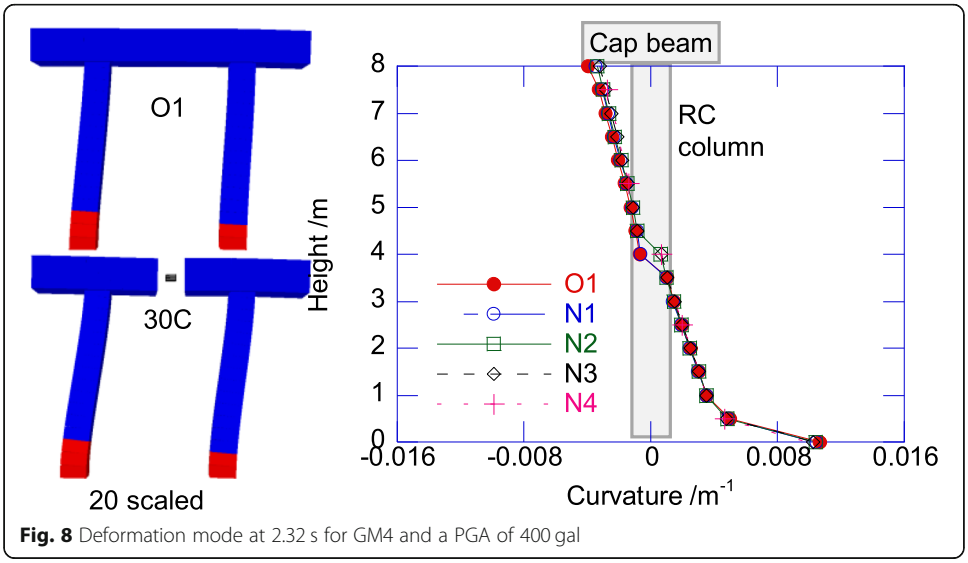

Fig. 8 Deformation mode at 2.32 s for GM4 and a PGA of 400 gal

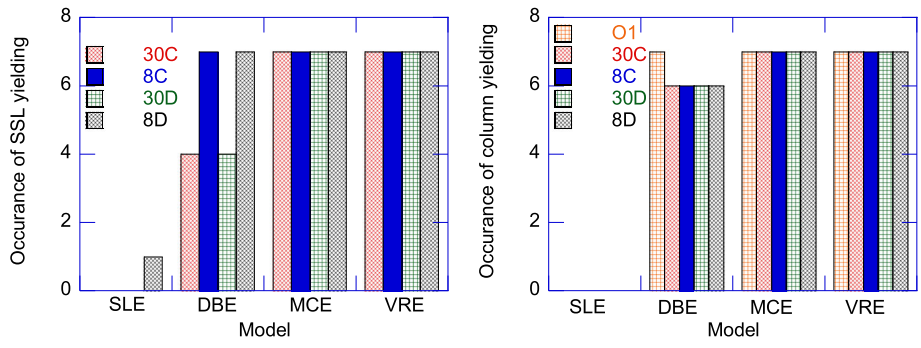

Fig. 9 Statistics of yielding occurrence

5.2 SSL performance

The peak shear force in the cap beam is presented in Fig. 12. It is obvious that the shear force is strongest for O1 and weakest for 8C. The shear force in the cap beam does not obviously increase when the earthquake intensity increases from the MCE to the VRE. After the yielding of the SSL and bottom section of the RC column, the internal force, including the shear force in the cap beam, does not evidently increase when the structure of the twin-column pier becomes flexible with adequate plastic hinges. For novel piers, the peak shear forces are not proportional to the web thickness of the SSL. According to Fig. 8, the SSL withstands axial tension when there is a height difference for two cap beams. Additionally, the axial tensile force of the SSL transfers a shear force to the cap beam. The shear force in the cap beam is determined by the coupled tensile-shear capacity of the SSL. Moreover, the cap beam in 30D experiences a stronger shear force than that in 30C. This result indicates that the continuous main girder transfers a shear force between two columns.

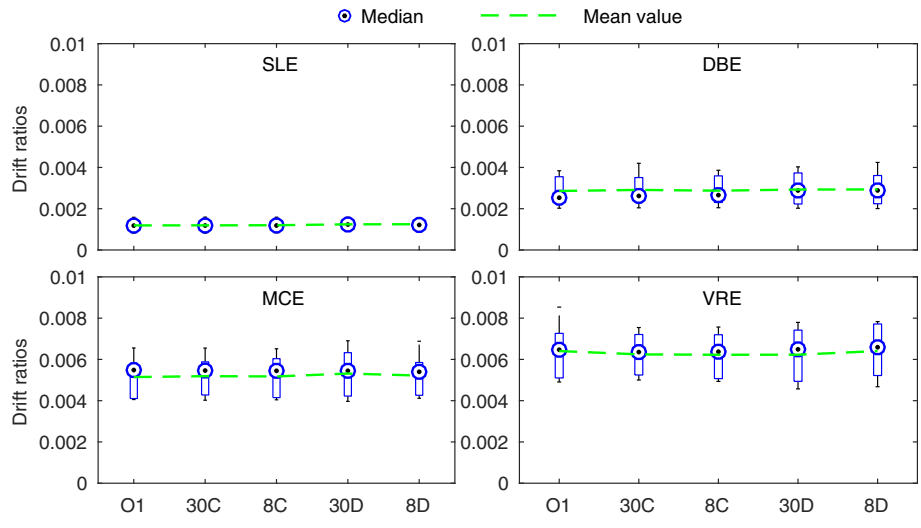

Fig. 10 Comparison of maximum transverse drift ratios

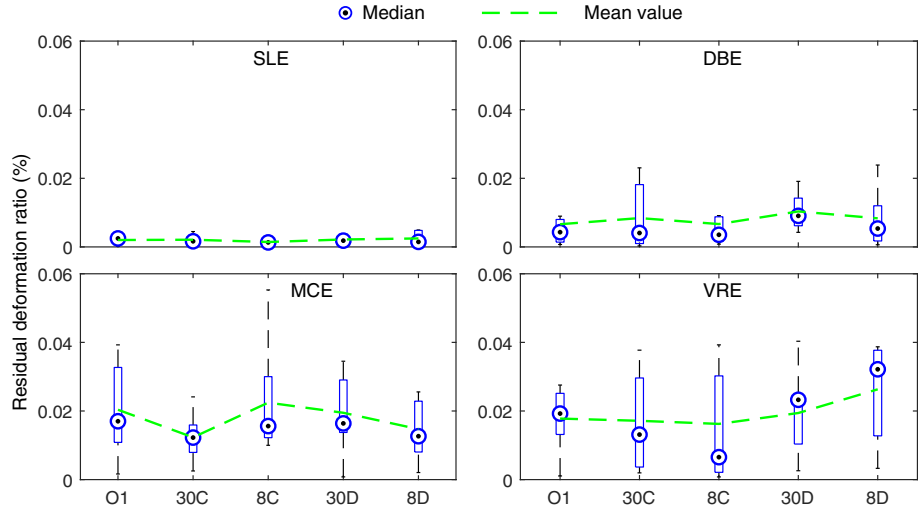

Fig. 11 Residual deformation of twin-column pier

The ratio of the energy dissipated by the two SSLs to the total input seismic energy is presented in Fig. 13. Energy dissipation ratios are negligible at the SLE intensity. The SSLs dissipate certain amounts of energy at DEB, MCE, and VRE intensities. Eight-millimeter-thick SSLs dissipate more energy than 30-mm-thick SSLs, benefitting from the earlier yielding mechanism. Because the continuous main girder weakens the decoupled deformation of the two RC columns, 30D and 8D have a larger energy dissipation ratio than 30C and 8C. The plasticity of the SSL thus develops less when there is a continuous main girder. It is noteworthy that the maximum energy dissipation ratio of 8D is only 1.3×10^{-3} among all intensities. Such low energy dissipation hardly contributes to the overall structural damping ratio of the bridge. Most input energy is still dissipated by natural damping, the hysteretic performance of bearings, and the plastic deformation of RC columns. Thus, considering the unchanged mass distribution and

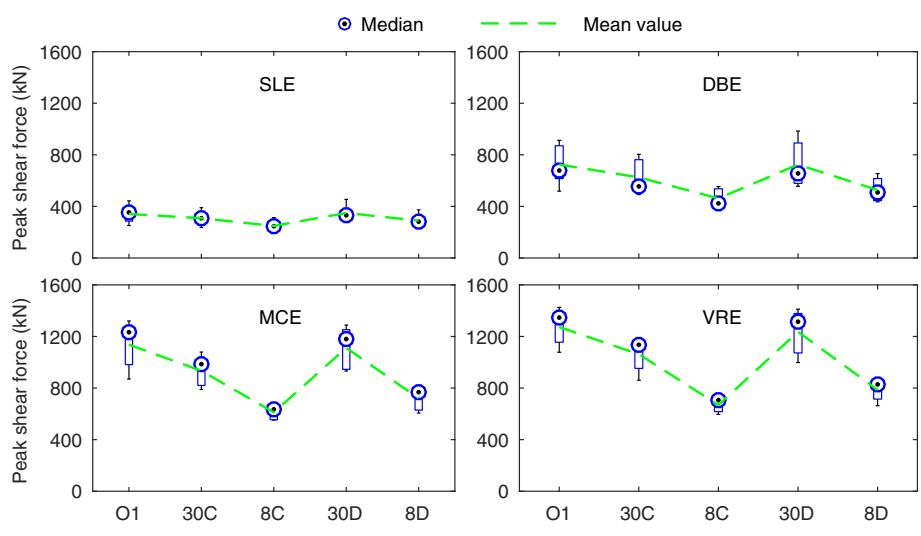

Fig. 12 Peak shear force for the cap beam

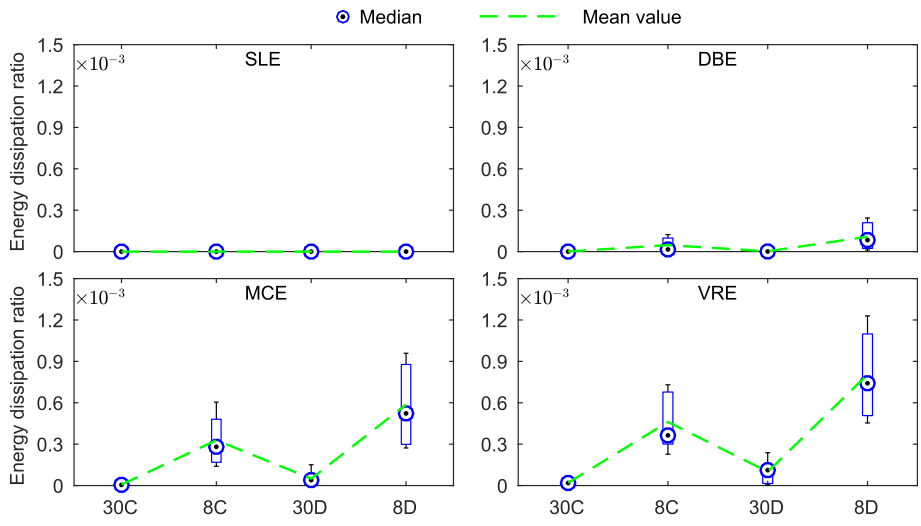

Fig. 13 Energy input and dissipation

natural periods, the macro responses (e.g., the deformation pattern and maximum transverse drift) are unaffected by introducing the SSL to the cap beam.

5.3 Damage control

Damage to RC piers is indicated by strain acting on the RC columns. The peak tensile and compressive strains of RC columns are compared in Fig. 14a and b respectively. Introducing the SSL does not visibly affect the peak tensile strain at SLE and DBE intensities. Meanwhile, 30C has much lower peak tensile strain than O1 at MCE and VRE intensities; that is, reductions of nearly 26.4%. The yielding of the SSL limits the peak value of the axial tensile force in one column, reducing the peak tensile strain. At SLE and DBE intensities, the limitation effect on the axial tensile force is not evident. There is thus no evident corresponding tensile strain reduction.

Peak compressive strains are also evidently reduced by the SSL at DBE, MCE, and VER intensities. As an example, the average value of the peak compressive stain in 30C is 18.6 and 17.1% lower than that in O1 at MCE and VRE intensities, respectively. The other three models also outperform O1 in controlling the peak compressive strain. These results show the realization of compressive damage control. Furthermore, 8C reduces damage best among models at the DBE intensity while 30C performs best among models at MCE and VRE intensities. Similar to the case for many other passive energy dissipation devices, the optimal strength of the SSL in the cap beam in the twin-column pier varies with the earthquake intensity or lateral drift. The weaker SSL has better control performance at lower intensity, while a stronger SSL is needed when the target intensity is higher.

Note that 30C outperforms 30D in terms of reducing damage. The mechanism of the continuity of the main girder is shown in Fig. 15. With a continuous main girder, two bearings may subjected to the different compressive load owing to the lateral constraint from the rigid diaphragm. The imbalanced vertical load generates a restoring moment at the column top, and this moment is opposite the bending moment at the bottom of

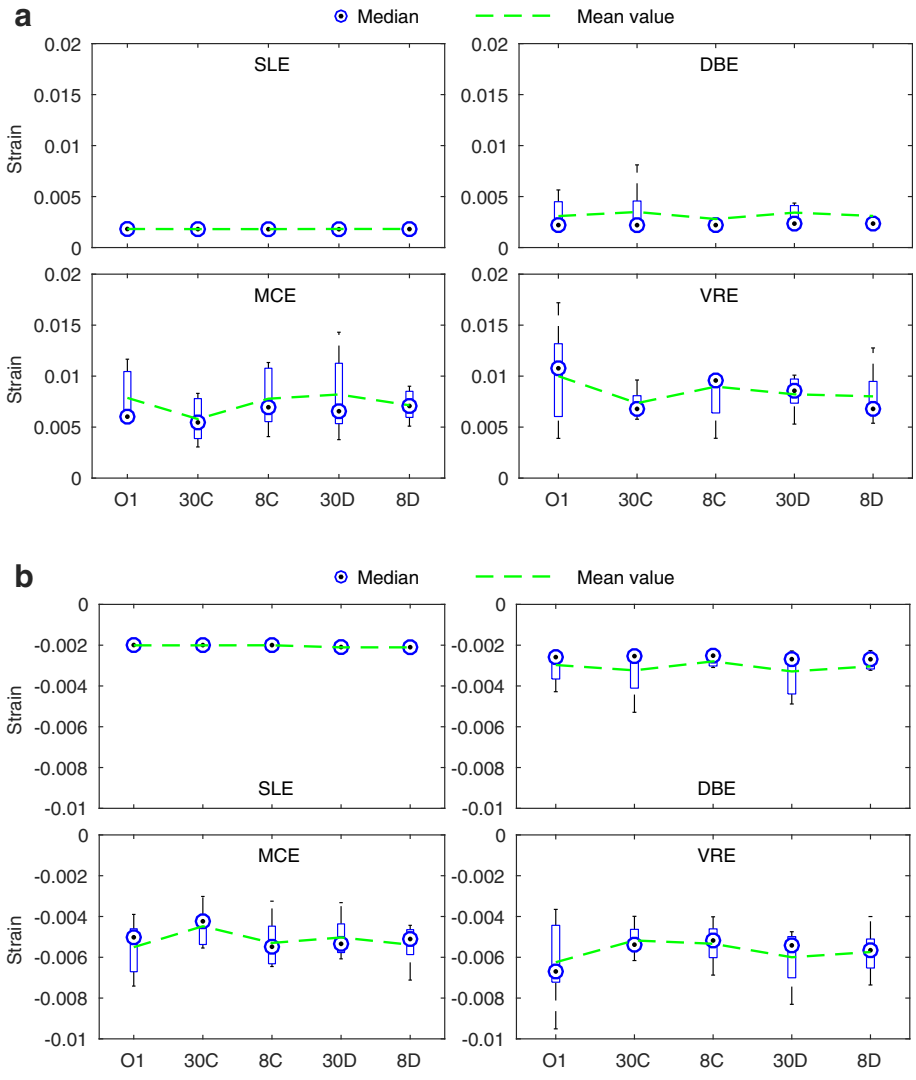

Fig. 14 Comparison of peak strain in a twin-column pier

the column. The moment at the bottom of the column can be further reduced. Therefore, the discontinuous main girder can deform in a manner coordinated with deformation of the interrupted cap beam, and the entire bearing uniformly shares the gravity load. There is no extra restoring moment at the column top.

Following the above concept, the middle wet joint of the discontinuous main girder may be subject to coupled bending–tension deformation. The peak cumulative plastic strain (*CPS*) of the middle wet joint is shown in Fig. 16. Little difference is seen at SLE and DBE intensities. At MCE and VRE intensities, 30D and 8D, with a discontinuous main girder, deliver much larger *CPS* than 30C and 8C. Without the rigid diaphragm, more deformation concentrates on the middle wet joint in the event of an earthquake owing to the deformation compatibility with the cap beam. The accompanied transverse bending at the middle wet joint thus leads to the development plastic strain. A continuous main girder is recommended to reduce compressive strain and control damage to the main girder.

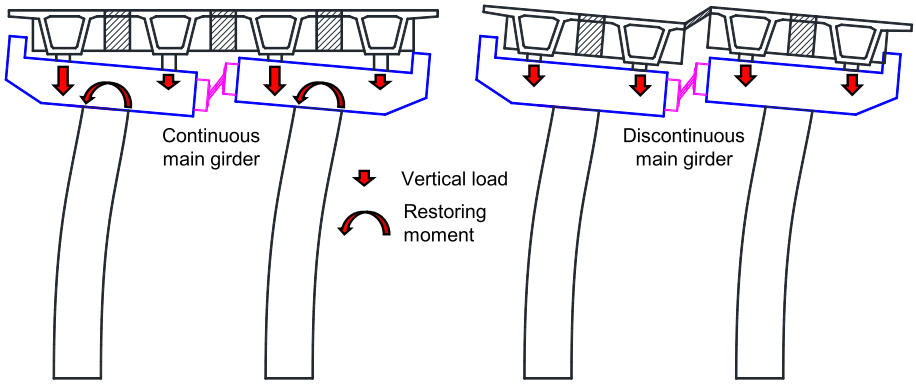

Fig. 15 Effect of the transverse continuity of the main girder

6 Conclusion

This paper proposed a novel twin-column pier with a replaceable SSL for damage control in the event of transverse seismic motion. A benchmark RC bridge was employed in nonlinear dynamic analysis for the quantitative comparison of damage control when introducing the SSL. The strength of the SSL and the transverse continuity of the main girder were considered parameters in the analysis. Results revealed that introducing the SSL in the cap beam reduced the compressive strain at the bottom of the RC column, while there was little reduction of the macro seismic response. The main findings of the study are as follows.

1) The peak compressive strain was reduced by 18.6 and 17.1% respectively when introducing the SSL in the cap beam at MCE and VRE intensities. There was no evident damage reduction at low intensities. When using an SSL, the design should avoid the crushing of concrete in the event of a strong earthquake.
2) The energy dissipated by SSLs was less than 0.13% of the total input energy. Natural periods were not evidently affected by introducing an SSL. There was thus

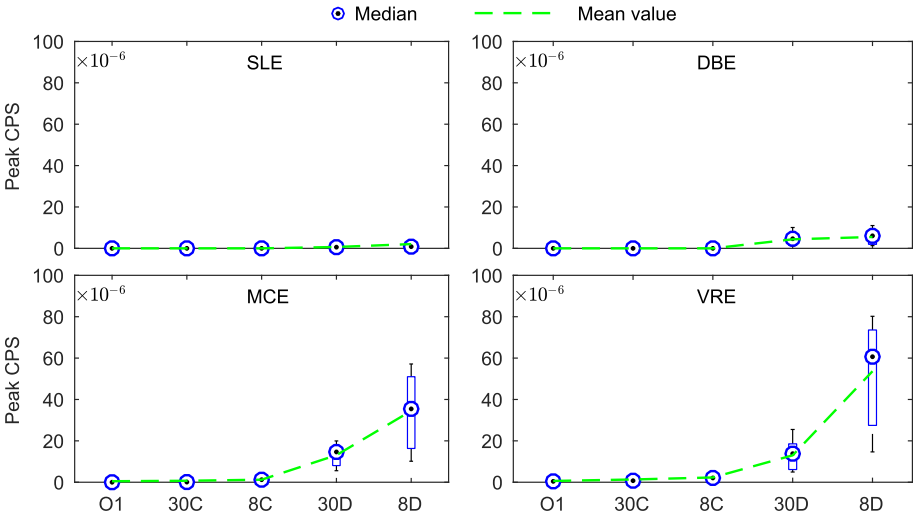

Fig. 16 Peak *CPS* of the middle wet joint in the main girder

little difference in the macro structural response. The damage control mechanism mainly related to a change in the deformation pattern.

3) The adoption of a transverse continuous main girder is suggested as it provides an additional restoring moment at the column top, which reduces the moment at the column bottom.

Abbreviations

SSL: Steel Shear Link; RC: Reinforced Concrete; PTFE: Polytetrafluoroethylene; EP: Elastomeric Pad; GM: Ground Motion; SLE: Service Level Earthquake; DBE: Design-Based Earthquake; MCE: Maximum Considered Earthquake; VRE: Very Rare Earthquake; CPS: Cumulative Plastic Strain

Acknowledgements

Not applicable.

Authors' contributions

Dr. Tengfei Xu contributed to the writing work. Mr. Xuemeng Bai contributed to the revision word. Mr. Weiting Chen performed the numerical analysis. Ms. Shanshan Ke performed the numerical analysis. Dr. Kailai Deng provided the idea and contributed to the writing work. Dr. Haiqing Xie provided some consulting suggestion to the analysis and figure drawing. The author(s) read and approved the final manuscript.

Funding

This study was supported by the National Natural Science Foundation of China (Grant No. 52078436) and Sichuan Science and Technology Program (Grant No. 21CXTD0094).

Availability of data and materials

Some or all data, models, or code that support the findings of this study are available from the corresponding author upon reasonable request.

Competing interests

The authors declare that they have no competing interests.

Author details

[1]Department of Bridge Engineering, Southwest Jiaotong University, Chengdu 610031, China. [2]CCCC Highway Consultants Co. Ltd, Beijing 100088, China. [3]Sichuan Province Key Laboratory of Seismic Technology, Southwest Jiaotong University, Chengdu 610031, People's Republic of China. [4]China Railway Eryuan Engineering Group Co. Ltd, Chengdu 610031, China.

Received: 10 November 2020 Accepted: 27 December 2020
Published online: 02 April 2021

References

Abaqus (2015) V. 6.14, analysis user's manual. DS Simulia Corp., Johnston Online Documentation

Bhuiyan AR, Alam MS (2013) Seismic performance assessment of highway bridges equipped with superelastic shape memory alloy-based laminated rubber isolation bearing. Eng Struct 49:396–407

Deng K, Pan P, Su Y, Ran T, Xue Y (2014b) Development of an energy dissipation restrainer for bridges using a steel shear panel. J Constr Steel Res 101:83–95

Deng K, Pan P, Sun J, Liu J, Xue Y (2014a) Shape optimization design of steel shear panel dampers. J Constr Steel Res 99:187–193

Deng K, Yan G, Yang H, Zhao C (2019b) RC arch bridge seismic performance evaluation by sectional NM interaction and coupling effect of brace beams. Eng Struct 183:18–29

Deng K, Zheng D, Yang C, Xu T (2019a) Experimental and analytical study of fully prefabricated damage-tolerant beam to column connection for earthquake-resilient frame. J Struct Eng 145(3):04018264

Dong H, Du X, Han Q, Hao H, Bi K, Wang X (2017) Performance of an innovative self-centering buckling restrained brace for mitigating seismic responses of bridge structures with double-column piers. Eng Struct 148:47–62

El-Bahey S, Bruneau M (2012) Bridge piers with structural fuses and bi-steel columns. I: experimental testing. J Bridg Eng 17(1):25–35

El-Tawil S, Harries KA, Fortney PJ, Shahrooz BM, Kurama Y (2010) Seismic design of hybrid coupled wall systems: state of the art. J Struct Eng 136(7):755–769

Gao X, Zhang Y (2013) Nonlinear analysis of a RC column under cycling loads. Struct Eng 30(3):56–63

Han Q, Du X, Liu J, Li Z, Li L, Zhao J (2009) Seismic damage of highway bridges during the 2008 Wenchuan earthquake. Earthq Eng Eng Vib 8(2):263–273

Ishibashi T, Tsukishima D (2009) Seismic damage of and seismic rehabilitation techniques for railway reinforced concrete structures. J Adv Concr Technol 7(3):287–296

Ji X, Liu D, Sun Y, Molina Hutt C (2017) Seismic performance assessment of a hybrid coupled wall system with replaceable steel coupling beams versus traditional RC coupling beams. Earthq Eng Struct Dyn 46(4):517–535

Li G (2010) Experimental study and numerical analysis on seismic performance of reinforced concrete bridge columns. Master Thesis, Chongqing Jiaotong University, Chongqing. (In Chinese)

Mansour N (2010) Development of the design of eccentrically braced frames with replaceable shear links. Doctoral dissertation, University of Toronto: Toronto

Ministry of Communications of the People's Republic of China (2004) Pad rubber bearing for highway bridge. Ministry of Communications of the People's Republic of China, Beijing (In Chinese)
Saatcioglu M, Razvi SR (1992) Strength and ductility of confined concrete. J Struct Eng 118(6):1590–1607
Shen X, Wang X, Ye Q, Ye A (2017) Seismic performance of transverse steel damper seismic system for long span bridges. Eng Struct 141:14–28
Taflanidis AA (2011) Optimal probabilistic design of seismic dampers for the protection of isolated bridges against near-fault seismic excitations. Eng Struct 33(12):3496–3508
Xu L, Li J (2014) Dual-level design method of sacrificial aseismic retainers. China J Highway Transp 28(10):59–66 (In Chinese)
Zhuang W, Chen L (2013) Analysis of highway's damage in the Wenchuan earthquake. China Communication Press, Beijing (In Chinese)

Publisher's Note